Proceedings World Geothermal Congress 2015
Melbourne, Australia, 19-25 April 2015

Radiogenic Heat Production and Heat Flow in Talca Basin (35.5°S), Central Chile

Mauricio Muñoz[1,2], Cristian Morales[1,2], Miguel Ángel Parada[1,2], Diego Morata[1,2], Valentina Flores[1,2], Gabriel Vargas[1,2], Sofía Rebolledo[1]

[1]Departamento de Geología, FCFM, Universidad de Chile, Plaza Ercilla 803, Santiago, Chile

[2]Centro de Excelencia en Geotermia de los Andes (CEGA), FCFM, Universidad de Chile, Plaza Ercilla 803, Santiago, Chile

E-mail: maumunoz@ing.uchile.cl

Keywords: Talca basin, radiogenic heat production, heat flow

ABSTRACT

The aim of this work is to determine the influence of the Radiogenic Heat Production (RHP) of lithospheric rocks in the heat flow coming up from rock basement, beneath Talca basin, located between Coastal Range and Andean Range. The RHP is estimated based on the content of Radiogenic Heat Production Elements (RHPEs: U, Th and K) of lithologies, which compose the lithosphere beneath Talca. The concentration of RHPEs is measured in distributed Mesozoic and Cenozoic outcropping rocks, using a portable gamma ray spectrometer. The RHPEs for middle, and lower crust are estimated by extending beneath the Talca basin, the Paleozoic coastal metamorphic complex, and by inferring the presence of granulites, respectively. Physical properties of lithospheric mantle are taken from petrological and geophysical studies. The thermal structure of lithosphere is performed in a 2-D lithospheric cross-section, with a finite elements modelling of heat transfer in solids with COMSOL multiphysics. The model was performed considering the RHP as a heat source of each lithospheric unit, temperature as a thermal boundary conditions at the top and bottom of lithosphere, and its architecture, which is determined from an upper crust deformation model, and geophysical data from deeper lithospheric units. The estimated heat flow, which reaches the basin floor, from rock basement in Talca basin is 62-65 mW/m^2.

1. INTRODUCTION

The heat flow that reaches the surface from the rock basement is a heat source for geothermal researches, especially in low-enthalpy geothermal resources. In central Chile there are just few conventional heat flow determinations, and there is not estimation of its variation across east-west profiles considering petrophysical parameters, lithospheric architecture, and geodynamic scenarios. The two conventional estimations of heat flow, indicate 60.7 and 78.7 mW/m^2 for Andean Range and Coastal Range, respectively (Uyeda et al., 1978). In addition, there are some continuous estimations of heat flow based on interpolation of discrete data (Hamza and Muñoz, 1996; Hamza et al., 2005), but lack of enough data produces uncertainties.

The purpose of this work is to establish a continuous heat flow coming up from rock basement along an east-west profile, consequent with the geological setting beneath Talca basin. This heat flow is estimated by finite elements modelling of heat transfer in lithosphere. The main thermal input data for modelling are temperature at the top, and bottom of lithosphere, and Radiogenic Heat Production (RHP) of lithologies, which compose the lithosphere. The geophysical information and upper crust deformation models are used to constrain a profile for lithosphere architecture. Physical properties for units comprising the lithosphere are determined according to lithologies. Furthermore, some thermal properties were measured by this study.

2. GEOLOGY OF THE BASEMENT

Talca basin is located between Coastal Range by the west, and Andean Range by the east, in central Chile (Figure 1). This basin is mainly filled by gravel-sized fluvio-alluvial and fluvial deposits (Hauser, 1995). Pleistocene to Holocene pyroclastic deposits cover a wide area of the northern part of the basin (Figure 1).

The upper crust in Talca is composed by rock units from the Coastal Range, and western part of the Andean Range. The Coastal Range is composed of Paleozoic metamorphic rocks, and Jurassic intrusive rocks in the west, and Mesozoic volcanic rocks intruded by large Mesozoic granitic bodies in the east. The western part of the Andean Range is composed of Cenozoic volcanic rocks intruded by Miocene batholiths (Figure 1). A brief description of the main rock units of the upper crust from east to west is given below.

The Paleozoic metamorphic rocks located west of Coastal Range are grouped into two metamorphic series: Western and Eastern series (Gana and Hervé, 1983) that correspond to Miyashiro's (1961) model of paired metamorphic belts formed in an accretionary prism. The Eastern series is intruded by a large batholith interpreted as the roots of the coeval volcanic arc (Hervé, 1988). The marine sedimentary sequences, and volcanic formations of Upper Triassic-Lower Jurassic age (Belmar et al., 2003) overlie the western flank of the Paleozoic batholith. These formations host a north-south plutonic belt of Middle Jurassic tonalites and granodiorites (Munizaga and Hervé, 1973; Gana and Hervé, 1983).

The western flank of the Coastal Range is formed by an Upper Jurassic-Cretaceous volcano-sedimentary sequence, which includes El Laurel Strata, Cerro Caupolicán Ignimbrite, Litu Strata, and El Culenar Formation (Bravo, 2001), in addition to Cretaceous batholiths. Rocks of the eastern limit of the Talca basin correspond to the Abanico Formation, which is a continental volcanic-sedimentary sequence that occupies the western flank of the Andean Range.

The main structure of the eastern part of Talca basin is the San Ramón Fault System, which is a west verging reverse fault system, which controls the eastern edge of the basin (Armijo et al., 2010). The main Coastal Range structure is the Litu Fault System, which corresponds to a normal fault system of N10-15E direction (Bravo, 2001).

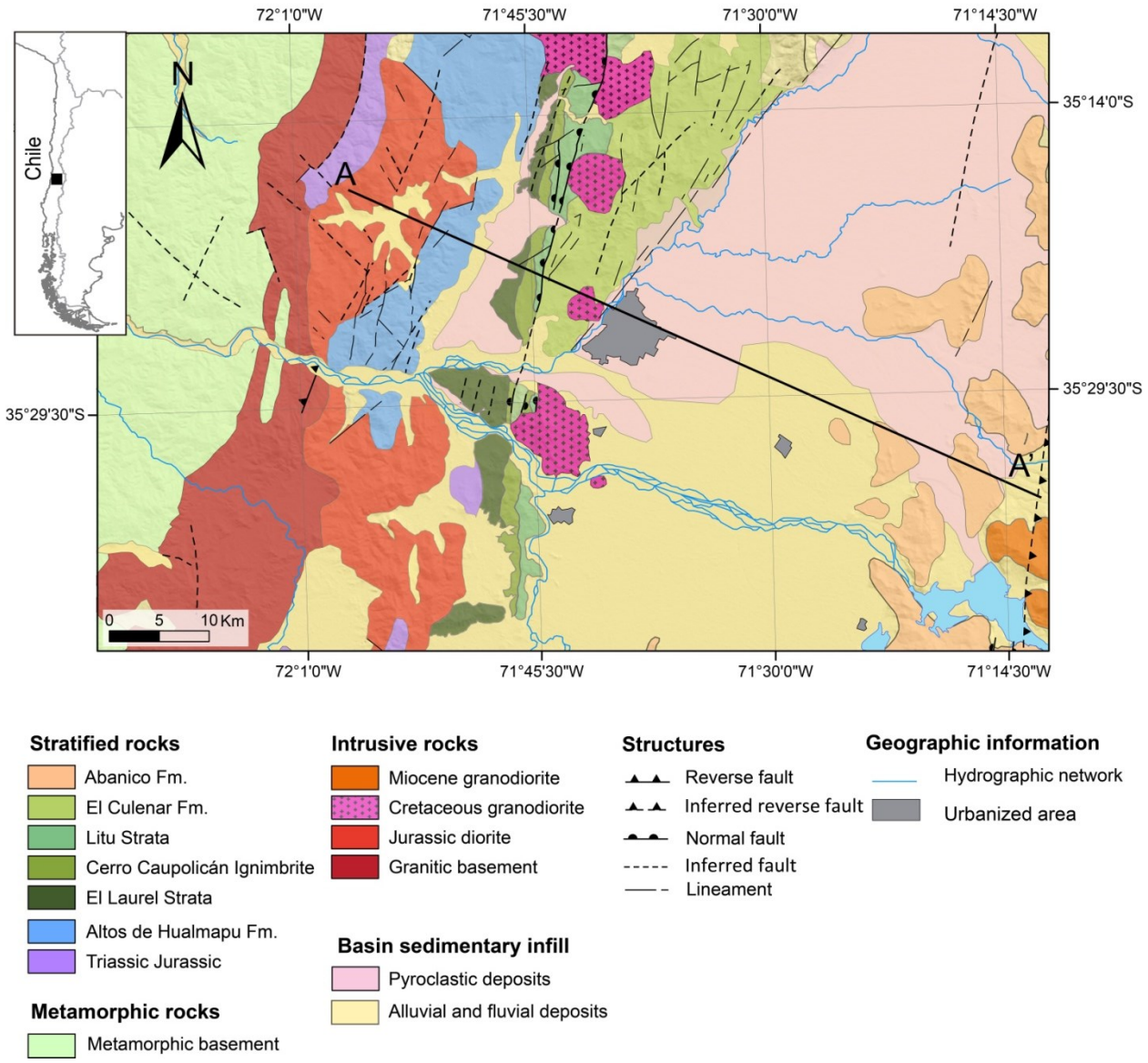

Figure 1: Geological map of Talca.

3. LITHOSPHERIC CONFIGURATION

The main boundaries within the continental lithosphere, and subducted slab were extracted from geophysical studies. The Mohorovičić discontinuity (Moho) was adjusted matching the local constraints given by refraction seismic profiles for regions near the trench axis, and short to intermediate wavelength Bouguer anomaly (Tassara, 2006; Tassara and Echaurren, 2012). The geometry, and depth of continental Lithosphere Asthenosphere Boundary (LAB) was fitted to intermediate to long wavelength Bouguer anomaly, in addition to continental scale seismic tomography models (Tassara, 2006; Tassara and Echaurren, 2012). The top of the Nazca slab has been imaged by reflection, and refraction seismic profiles along some regions of the fore arc, and hypocenters recorded by local seismic networks (Tassara, 2006; Tassara and Echaurren, 2012).

The continental crust was divided into three layers: upper, middle, and lower crust according to travel time tomography (Krawczyk et al., 2006; Moscoso et al., 2011). To constrain the upper continental crust geometry we used structural deformation models for the Coastal Range (Bravo, 2001), and Andean Range (Armijo et al., 2010).

In accordance to the top of subducted slab, and LAB depth the continental crust beneath the Talca basin is above the mantle wedge.

4. DATA BASE

Some physical properties, in particular thermal, are required to carry out the modelling of heat transfer in the lithosphere (Table 1). The density ρ was measured in the upper crust lithologies. For the remainder of lithosphere, its value is extracted from literature as a function of its composition (Tassara, 2006). Thermal conductivity k was taken from literature according to lithology, and expected temperature (He et al., 2009), as well as for the constant pressure heat capacity C_P (Robie, 1995; Merriman et al., 2013).

The Radiogenic Heat production (RHP), defined as the amount of heat released per unit time in a rock volume by the disintegration of radiogenic unstable isotopes (W/m^3), is obtained using the Rybach´s (1988) expression:

$$RHP = 10^{-5} \times \rho \times \left(9.52\, C_U + 2.56\, C_{Th} + 3.48\, C_K\right) \quad (1)$$

Here ρ is density (kg/m^3), C_U, C_{Th} and C_K are the concentrations of Uranium (ppm), Thorium (ppm), and Potassium (wt %), respectively. The RHP for geological units of upper crust is estimated from *in-situ* measurement of Radiogenic Heat Production Elements (RHPEs), while concentrations for deeper lithospheric rocks were extracted from literature (He et al., 2009).

Table 2: Physical and thermal properties for lithosphere beneath Talca basin.

Geologic Unit	ρ [kg/m^3]	C_P [J/kg·K]	k [4] [W/(m·K)]	RHP [μW/m^3]
Abanico Fm.	2540	800 [1]	2.9·(1/(1+0.0015·T))	0.4
El Culenar Fm.	2520	800 [1]	2.9·(1/(1+0.0015·T))	1.3
Litu Strata	2570	800 [1]	2.9·(1/(1+0.0015·T))	1.7
Cerro Caupolicán Fm.	2540	800 [1]	2.9·(1/(1+0.0015·T))	2.8
El Laurel Strata	2550	800 [1]	2.9·(1/(1+0.0015·T))	1
Hualmapu Fm.	2590	800 [1]	2.9·(1/(1+0.0015·T))	1.6
Trassic-Jurassic	2700	800 [1]	2.9·(1/(1+0.0015·T))	1.9
Createcous intrusive	2500	800 [1]	2.9·(1/(1+0.0015·T))	1.8
Jurassic intrusive	2640	800 [1]	2.9·(1/(1+0.0015·T))	2.3
Average upper crust	2600[3]	800 [1]	2.9·(1/(1+0.0015·T))	1.3
Middle crust	2700[3]	800 [1]	2.8·(1/(1+0.0015·T))	0.083 [4]
Lower crust	3100[3]	1000 [2]	2.5·(1/(1+0.0015·T))	0.037 [4]
Lithospheric mantle	3100[3]	$1617.4-0.021\cdot T-14047\cdot T^{-0.5}$ [5]	$3\cdot(1/(1+0.0001\cdot T)+3\cdot10^{-10}\cdot(T+273.15))^3$	0.02 [4]

[1](Robie, 1995), [2](Vosteen y Schellschmidt, 2003), [3](Tassara, 2006), [4](He et al., 2009), [5](Merriman et al., 2013)

5. NUMERICAL THERMAL MODELLING

The heat flow that reaches the surface beneath Talca basin sedimentary infill is obtained by a thermal modelling of heat transfer in a continental lithospheric profile. The heat transfer modelling is performed regarding physical properties, especially thermal for the lithologies involved, and fixed temperatures as boundary conditions for top and bottom of lithosphere. Density data of the basement rocks are measured from representative samples of the geological units using Archimedean method. The RHP is estimated from representative samples of the geological units established on its concentrations of RHPEs (U, Th and K). The concentrations of RHPEs are measured with a portable gamma-ray spectrometer (RS125, Radiation Solution Inc.). The procedure was 5 minutes each measurement (in accordance with manufacturer indications) and 3 to 5 samples per outcrop. Physical, especially thermal properties for the remainder of lithospheric constituents (middle and lower crust and mantle) are inferred from previous studies (Robie, 1995, Vosteen y Schellschmidt, 2003, Tassara, 2006; He et al., 2009, Merriman et al., 2013).

The modelling the heat transfer in the continental lithosphere is carried out with the solids module of COMSOL Multiphysics. Heat transfer in solids states the heat flow is determined by heat capacity at constant pressure, thermal gradient, thermal conductivity, and heat sources, as follow:

$$\rho c_P \frac{\partial T}{\partial t} + \nabla \cdot \left(-k \nabla T\right) = Q \quad (2)$$

Here, ρ is the density (kg/m^3), C_P is the specific heat capacity at constant pressure (J/(kg•K)), T is absolute temperature (K), k is thermal conductivity (W/(m•K)), and Q contains heat sources (W/m^3).

To incorporate the effect of heat transfer by radiation in lower continental lithospheric layers, where a high temperature is expected (>800ºC), we used modified expressions for heat capacity at constant pressure (Merriman et al., 2013), as well as for thermal conductivity (He et al., 2009).

5. RESULTS AND DISCUSSION

Thermal modelling of lithosphere heat transfer is performed based on geometry of the lithosphere, petrological setting described above, and thermal boundary conditions. On top of lithosphere is considered a constant temperature of 13ºC, whereas at the bottom of lithosphere is considered a linearly varying temperature between 940ºC in west, to 1070ºC in the east, according to thermal models performed in subduction zones (e.g. Manea et al 2005). Both edges of the model are considered thermally insulated.

The result of thermal modelling provide a heat flow that reaches the surface, beneath the basin sedimentary infill, ranges between 62 to 65 mW/m^2. The presence of major intrusive bodies in the upper crust increases the heat flow in 2 mW/m^2 (Fig. 2). The estimated heat flow implies that the thermal gradient for the first kilometers of upper crust is about 24°C/km.

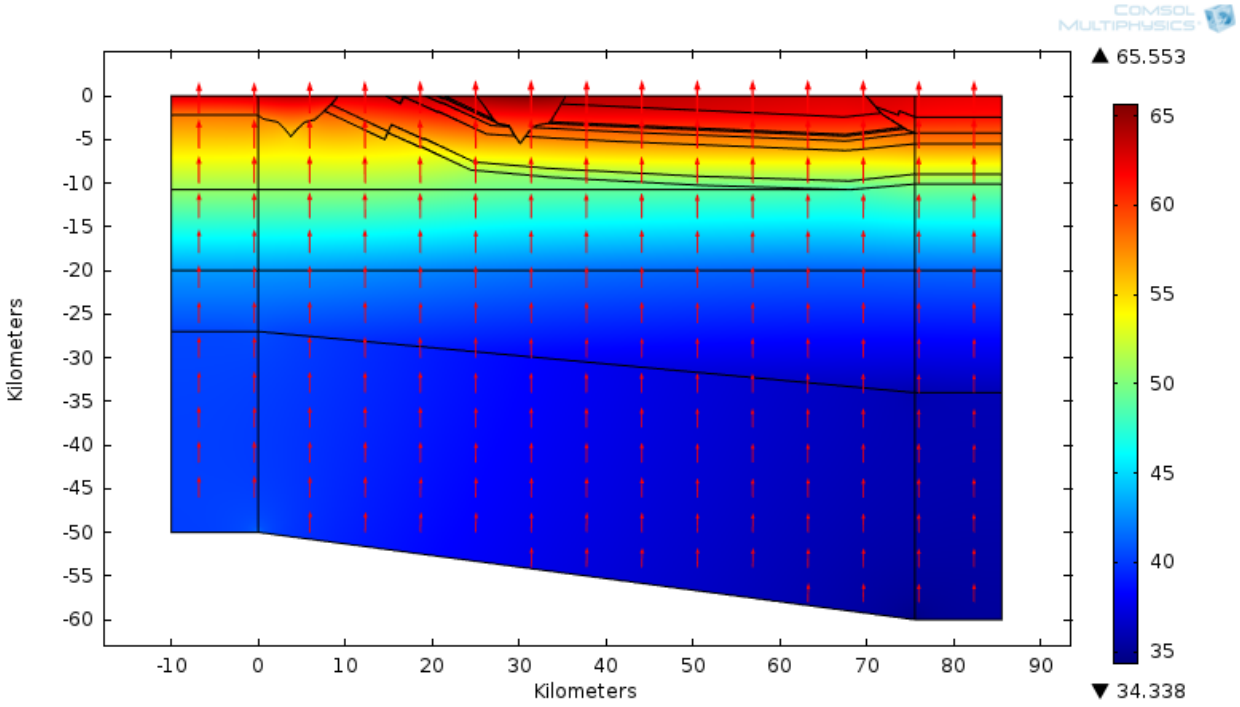

Figure 2: Total heat flow for continental lithosphere profile beneath Talca Basin. Profile A-A' in Figure 1.

From total heat flow that reaches the surface, 45 mW/m^2 are caused by temperature difference between the bottom and the top of lithosphere. Radiogenic heat production in the upper crust produces 13 mW/m^2, which represents 20% of resulting heat flow.

The RHP estimated for geologic units comprising the upper crust are consistent with expected values according to a world scale compilations based on lithology composition (Vilà et al., 2010).

The heat flow at the surface of 62-65 mW/m^2 is consequent with heat flow estimations in continental crust away from active volcanism (Mareschal and Jaupart, 2013).

6. CONCLUSION

The estimated heat flow that reaches the surface, coming up from rock basement, in the study area is 62-65 mW/m^2, which is consistent with petrophysical constraints, and lithospheric architecture beneath Talca basin. It is expected that this heat flow estimation will be similar for equivalent geological scenarios. Based on this heat flow estimation of 62-65 mW/m^2 and thermal conductivities expected in the range of 2.5 to 3 W/mK, the expected thermal gradient for the first kilometers below the surface without thermal disturbance will be approximately 24°C/km. In addition, the 20% of total heat flow that reaches the surface in Talca basin is produced by a radiogenic heat source in the upper crust.

ACKNOWLEDGMENTS

The authors would like to thank the FONDAP/CONICYT Nº 15090013 (Centro de Excelencia en Geotermia de los Andes, CEGA), Renewable Energy Division of the Chilean Energy Ministry, and Departamento de Geología, FCFM, Universidad de Chile.

REFERENCES

Armijo, R., Rauld, R. Thiele, Vargas, G., Campos, J., Lacassin, R. and Kausel E. Tectonics of the western front of the Andes and its relation with subduction processes: The San Ramón Fault and associated seismic hazard for Santiago (Chile), International Conference Montessus de Ballore-1906 Valparaiso Earthquake Centennial, Transaction ST1-03, Santiago, Chile (2010).

Belmar, M., Morata, D., Munizaga, F., Perez de Arce, C., Morales, S and Carrillo, F. J. Significance of K-Ar dating of very low-grade metamorphism in Triassic-Jurassic pelites from the Coastal Range of central Chile, *Clay Minerals*, **39** (2004), 151–162.

Bravo, P. Geología del Borde Oriental de la Cordillera de la Costa entre los Ríos Mataquito y Maule, VII Región, memory to achieve the title of geologist, Universidad de Chile (2001).

Gana, P and Hervé F. Geología del basamento cristalino en la Cordillera de la Costa entre los ríos Mataquito y Maule, VII Región, *Revista Geológica de Chile*, **19** (1983), 37-56.

Hamza V. and Muñoz, M. Heat Flow Map of South America, *Geothermics*, **25** (1996), 599-646.

Hamza, V. Silva, F., Gomes, A., Delgadilho, Z. Numerical and functional representations of regional heat flow in South America, *Physics of the Earth and Planetary Interiors*, **152** (2005) 223–256

Hauser, A. Carta Hidrogeológica de Chile N° 2, Hoja Talca, VII Región. Servicio Nacional de Geología y Minería, Santiago (1995).

He, L., Hu, S., Yang, W., y Wang, J. Radiogenic heat production in the lithosphere of sulu ultrahigh-pressure metamorphic belt. *Earth and Planetary Science Letters*, **277** (2009), 525–538.

Hervé, F. Late Paleozoic subduction and accretion in southern Chile. *Episodes*, **11** (1988), 183-188.

Krawczyk, C., Mechie, J., Lüth, L., Tašárová, Z., Wigger, P., Stiller, M., Brasse, H., Echtler, H. P., Araneda, M., and Bataille. K. Geophysical Signatures and Active Tectonics at the South-Central Chilean Margin. In Oncken, O., Chong, G., Franz, G., Giese, P., Götze, H. J., Ramos, V., Strecker, M., and Wigger, P., editors, The Andes, Active Subduction Orogeny, Series: Frontiers in Earth Sciences (2006), 171-192.

Manea, V., Manea, M., Kostoglodov, V and Sewell, G. Thermo-mechanical model of the mantle wedge in Central Mexican subduction zone and a blob tracing approach for the magma transport. *Physics of the Earth and Planetary Interiors*, **149** (2004), 165–186.

Mareschal, J. C. and Jaupart, C. Radiogenic heat production, thermal regime and evolution of continental crust, *Tectonophysics*, **609** (2013), 524-534.

Merriman, J. D., Whittington, A. G., Hofmeister, A. M., Nabelek, P. I., and Benn, K. Thermal transport properties of major archean rock types to high temperature and implications for cratonic geotherms, *Precambrian Research*, **233** (2013), 358-372.

Miyashiro, A. Evolution of metamorphic belts, *Journal of Petrology*, **2** (1961), 277-311.

Merriman, J. D., Whittington, A. G., Hofmeister, A. M., Nabelek, P. I., and Benn, K. Thermal transport properties of major archean rock types to high temperature and implications for cratonic geotherms, *Precambrian Research*, **233** (2013), 358-372.

Munizaga, F., Aguirre, L. and Hervé, F. Rb/Sr ages of rocks from the Chilean metamorphic basement. Earth and Planetary Scence Letters, **18** (1973), 87-91.

Rybach, L. Determination of heat production rate, Handbook of Terrestrial Heat Flow Density Determination (1988), 486p.

Tassara, A. Factors controlling the crustal density structure underneath active continental margins with implications for their evolution, *Geochemistry Geophysics Geosystems*, **7** (2006), 21p.

Tassara, A. y Echaurren, A. Anatomy of the Andean subduction zone: three-dimensional density model upgraded and compared against global-scale models, *Geophysical Journal International*, **189** (2012), 161-168.

Robie, R. and Hemingway, B. Thermodynamic properties of minerals and related substances at 298.15 k and 1 bar (10^5 pascals) pressure and at higher temperatures. USGS Bulletin 2131 (1995).

Uyeda, S., Watanabe, T., Kausel, E., Kubo, M. and Yashiro, Y. Report of Heat Flow Measurements in Chile, *Bulletin of Earthquake Research Institute,* University of Tokyo, **53** (1978), 131-163.

Vosteen, H. D. and Schellschmidt, R. Influence of temperature on thermal conductivity, thermal capacity and thermal diffusivity for different types of rock, *Physics and Chemistry of the Earth*, **28** (2003) 499–509.

Vilà, M., Fernández, M., and Jiménez-Munt, I. Radiogenic heat production variability of some common lithological groups and its significance to lithospheric thermal modeling. *Tectonophysics*, **490** (2010), 152 - 164.